TRANSPORT PROPERTIES OF KIMBERLITE MELT

J.K. Russell[1], Daniele Giordano[4], Maya Kopylova[2], Stephen Moss[1,3]

[1]Volcanology Laboratory, [2]Diamond Exploration Laboratory, [3]Mineral Deposits Research Unit, Earth & Ocean Sciences, University of British Columbia, Canada; [4]Geological Sciences Department, Third University of Rome, Largo S. Leonardo Murialdo, 1, 00154 Rome, Italy

INTRODUCTION

The physical-chemical properties of kimberlite melt govern the transport and eruption behaviour of kimberlite magmas. However, the physical properties of kimberlitic melts remain unknown, in part, because the composition of the melt phase is poorly constrained (Price et al. 2000; Kopylova et al. 2006; Sparks et al. 2006). As well, the experimental techniques needed to probe these extreme melts for viscosity (η), glass transition temperatures (Tg), heat capacity (Cp), and volatile solubilities are not yet available. Furthermore, the physical properties of kimberlite melts need not be simple linear extrapolations from the properties of other silicate melts (Russell & Giordano 2005). Computational models, calibrated on high quality experimental data, provide a means of exploring the physical properties of silicate melts for which there are no data.

In this presentation we use the current estimates for the range of kimberlite melt compositions (Table 1 & 2; after Price et al. 2000; Sparks et al. 2006; Kopylova et al. 2006). Secondly, we introduce and apply two multicomponent chemical models for predicting specific physical properties of melts in general. These models are designed to predict the calorimetric glass transition temperature and the viscosity of silicate melts as a function of melt composition and are used to explore the corresponding properties of kimberlite melts.

PRIMARY KIMBERLITE MELT

Chemical compositions of primary kimberlite melt are difficult to isolate because kimberlite is a hybrid rock representing a mixture of mantle and crustal xenoliths, macrocrysts, and subordinate amounts of cognate phenocrysts and groundmass material (Mitchell, 1986). Kimberlites are also enriched in volatiles which can have post-eruption consequences. Even where kimberlite melt has been quenched, post-eruption circulation of fluids can cause changes in bulk chemistry, replacement of primary minerals, and obliteration of primary textures and structures (Price et al. 2000; Sparks et al. 2006).

Tables 1 & 2 report a suite of chemical compositions that purport to represent kimberlite melts and include: i) original analyses of Price et al. (2000), ii) compositions compiled by Sparks et al. (2006), and iii) new compositions from Kopylova et al (2006). As a group, the estimates derive from fine-grained aphanitic samples of kimberlite from the margins of dykes, melt compositions corrected for olivine accumulation, and reconstructed melt compositions from pyroclasts. They show a fair degree of agreement; on a normalized anhydrous basis they contain 30-36 wt. % SiO2, 25-36 wt. % MgO, 12-22 wt. % CaO, 8-14 wt. % FeO, and 1-2.5 wt. % K2O. CaO shows the greatest variation.

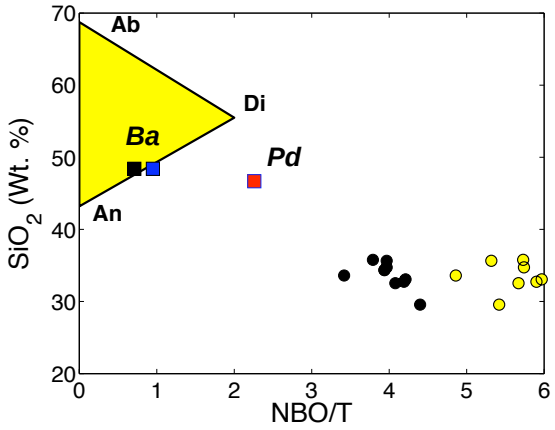

Fig. 1. Melt compositions plotted as NBO/T vs. Wt. % SiO_2 for: kimberlite (circles: black - anhydrous; yellow – hydrous), basalt (squares: blue – hydrous), peridotite (red square). The field for Di-An-Ab melts is shown for reference.

Kimberlite melts are expected to be volatile-rich and to contain both CO_2 and H_2O. The exact percentages of these two constituents remains largely uncertain because kimberlite glass does not exist, kimberlite rocks are nearly always affected by late-stage fluid infiltration (and attendant hydration-carbonation reactions), and many of the textures involving carbonate and hydrous phases are ambiguous in terms of separating melt or fluid crystallization processes.

Values of NBO/T (number of non-bridging oxygens per tetrahedra) have been calculated (Mysen 1988) as a means of comparing the range of kimberlite melt compositions to other melts (Tables 1, 2). Kimberlite melts feature very high values of NBO/T (3-4.4) relative to other silicate melts (Fig. 1), suggesting that kimberlite melts are highly depolymerized. The addition of H_2O causes even higher values of NBO/T (5-6). Synthetic melts of albite (Ab), anorthite (An), and diopside (Di) have a total range of 0 to 2 and are commonly viewed as rheological proxies for rhyolite (albite) and basalt (diopside) (Fig. 1). Basalt (dry and hydrous) melts, described by Giordano & Dingwell (2003), plot between An and Di. Peridotite melts synthesized by Dingwell et al. (2004) have high NBO/T values but remain substantially lower than kimberlite melts. Even anhydrous kimberlite melts have anomalously high NBO/T. This suggests that these melts are very fragile (e.g., Plazek & Ngai 1991) and should show non-Arrhenian temperature dependencies, although the effects of dissolved H_2O and CO_2 may reduce melt fragility (Giordano & Russell, *in review*). Furthermore, increasing NBO/T commonly correlates with reduced activation energies and reduced glass transition temperatures.

GLASS TRANSITION TEMPERATURE (Tg)

Naturally-occurring silicate glasses form under a variety of geological conditions and commonly form the main constituent in silicic volcanic rocks and in rapidly cooled mafic rocks. Kimberlite is unique in that there are no occurrences of kimberlite glass: this raises the question of whether glass ever forms in kimberlite eruption?

The glass transition temperature (Tg) marks the transition from the liquid to the glassy state. Glass formation is a boundary between changing environmental states. Above Tg, rates of nucleation, crystallization and vesiculation are sufficiently fast to drive magmatic processes. Conversely, where the liquid line of descent (T-X_{Melt} path) intersects the Tg of the melt, glass forms and these magmatic processes effectively cease.

Here we present an empirical model of predicting the thermodynamic glass transition temperature (Tg) as a function of melt composition. Operationally, the model produces T-dependent expressions for the heat contents of a silicate melt and glass of known composition. Intersecting heat content curves for glass and melt define Tg values (Fig. 2). The model is based on experimental heat content (N=500) and differential scanning calorimetric (DSC) heat capacity (N=250) measurements on silicate melts (>60) and glasses (>30). The model allows for tracking (T_{Magma}-Tg) and can indicate favourable conditions for glass formation (Fig. 3).

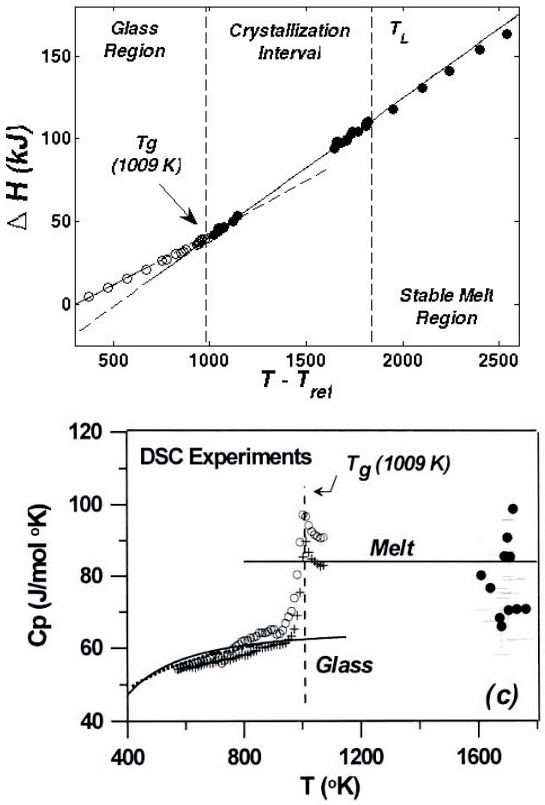

Fig. 2. Upper: Heat content curves for Di melts/glasses; intersection defines calorimetric Tg (736 °C). Lower: Peak in DSC heat capacity curve defines same Tg.

VOLATILES: CAVEAT EMPTOR

The major imitation to this model for calorimetric Tg is that the experimental database does not include heat content measurements on hydrous melts. Most silicate melts show large drops (100-250 °C) in characteristic Tg values with increasing H_2O contents. Thus, the Tg model provides a maximum T for glass formation because it cannot predict the Tg depression caused by dissolved volatiles (Fig. 4). Future work will modify the heat content equations to account for dissolved volatiles.

Tg SUMMARY

Glass formation depends on the gap between T_{Liq} and T_g and rates of melt cooling (Fig. 3). Below, we use

the calculated physical properties (e.g., viscosity and Tg) to explore the conditions required to produce quenched or glassy pyroclastic deposits of kimberlite and the potential for welding of these deposits (e.g., Quane & Russell, 2005). If kimberlite melt forms glass, then welded pyroclastic materials are expected within the conduit and in proximal extra-crater deposits. If kimberlite melt by-passes glass formation by forming a microcrystalline mesostasis, there remains the opportunity for hot-pressing of this fragmental material to produce an annealed, homogenous, apparently massive deposit. Both processes can operate effectively on a 10's of minutes to hours time-scale (Russell & Quane, 2005).

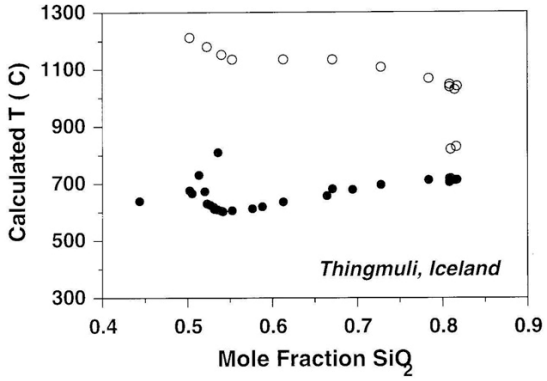

Fig. 3. Computed values of T_{Liq} (open) and Tg (closed) for picrite to rhyolite rocks from Thingmuli. Where T_{Liq} ~ Tg small degrees of undercooling promote glass formation.

KIMBERLITE MELT VISCOSITY

Melt viscosity is a critical physical property in volcanic systems as it governs styles and rates of eruption, rates of vesiculation and crystallization, and, ultimately, sets limits on coherent flow (vs. fragmented or disrupted flow). Here we use a new calculational model for silicate melt viscosity (Giordano & Russell, *in review*) to explore the properties of kimberlite melts.

The model uses the VFT equation [$\log \eta = A + B/(T(K) - C)$] to handle non-Arrhenian melt and has the following strengths: i) it spans most of the compositional range found in naturally-occurring volcanic rocks, ii) it models the effects of 10 major and minor oxide components and the volatile components H_2O and F, iii) it is computationally continuous across the entire compositional and temperature spectrum of the database, iv) it models both *strong* (near-Arrhenian) and *fragile* (non-Arrhenian) behaviour of silicate melts, and v) it reproduces expected relationships between melt composition and values of Tg and fragility (*m*). The model reproduces, to within measurement error, experimental values of viscosity for melts pertinent to kimberlite (Fig. 4).

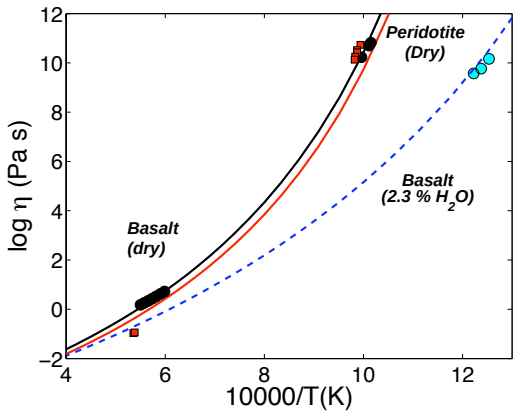

Fig. 4. Computed viscosities (solid lines) are compared to direct measurements for basalt (dry and wet) and peridotite melts (see Table 1 for sources).

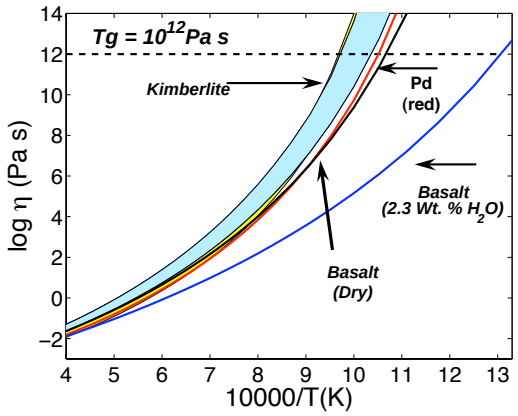

Fig. 5. Viscosity of kimberlite melts. Computed values of log η vs 10000/T(K) for kimberlite melts from Table 1 (dry- yellow) and Table 2 (hydrous – blue). Also shows computed curves for peridotite & basalt (see Fig. 4).

Values of viscosity are computed for the kimberlite melt compositions (Tables 1 & 2) although our model does not yet accommodate CO_2. The VFT equations for each melt are reported in Tables 1 & 2 along with the value of log η at 1200 °C.

We also report the rheological glass transition and melt fragility (m) given by the steepness index (Plazek & Ngai 1991). The rheological Tg is the temperature at which the melt attains a viscosity of 10^{12} Pa s and agrees well with the calorimetric Tg (Fig. 6). This correspondence between calorimetric and rheological Tg allows us to

use the viscosity model to compute Tg values for volatile-bearing (H_2O only) kimberlite.

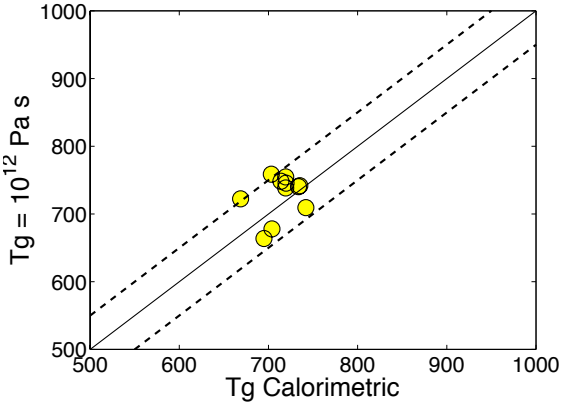

Fig. 6. Comparison of rheological and calorimetric values of Tg. Dashed lines denote +/- 50 °C.

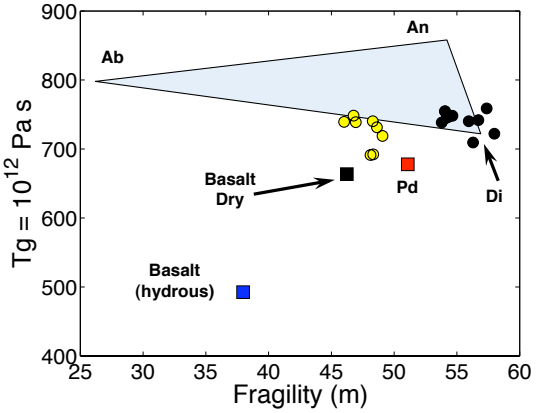

Fig. 7. Computed values of *m* and Tg for dry (black) and hydrous (yellow) kimberlite.

Kimberlite melts show virtually no decrease in *Tg* (K) with increasing H_2O contents. This contrasts the behaviour of basaltic melts; as shown by Giordano & Dingwell (2003) 2.3 wt. % H_2O causes a 200 °C depression of Tg (Fig. 7). Normally the depression of Tg with increased H_2O content provides a simple vehicle for production of glass during an eruption. Ascent and eruption causes volatile loss and a concomitant increase in Tg to the point that Tg rises to meet the T_{magma}. At this point melt is quenched to glass. Kimberlite melts do not show the same depression in Tg and, thus, lack this means of aiding glass formation. In addition, the ΔT between T_{magma} and Tg is higher than in many other magmas (Fig. 8).

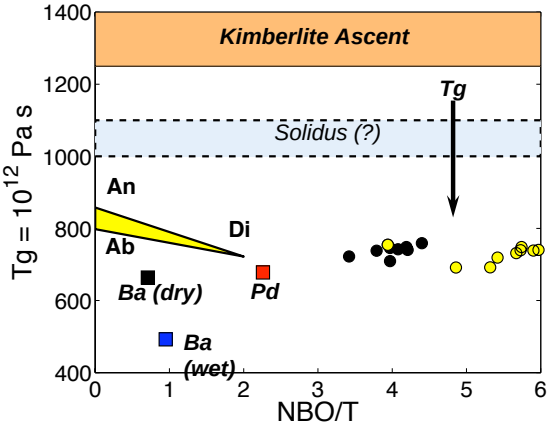

Fig. 8. The Tg(°C) for kimberlite melts as a function of NBO/T. Tg values lie well below formation temperatures. Glass formation requires 300 °C cooling below solidus T and 400-600 °C cooling below formation T.

In contrast, fragility (*m*) decreases with increasing H_2O content which parallels the behaviour seen in most silicate melts. As discussed by Giordano & Russell (*in review*), volatiles reduce fragility and the effect is greatest for the most fragile melts (e.g., kimberlite) and least for strong melts (e.g., rhyolite).

Acknowledgements

We thank Diavik Diamond Mines, Inc. (DDMI) and the Natural Sciences and Engineering Research Council (NSERC) for their financial and logistical support.

References Cited

Dingwell D Courtial P Giordano D & Nichols A 2004 Viscosity of peridotite liquid. EPSL, 226: 127-138.

Giordano D & Dingwell DB 2003. Viscosity of hydrous Etna basalt: implications for Plinian-style basaltic eruptions. Bull Volcanol. 65: 8-14.

Giordano D & Russell JK 2006. Viscosity and fragility of natural (volatile-bearing) magmas. Nature, Submitted 08/06.

Kopylova MG Matveev S & Raudsepp M 2006. Searching for primary kimberlite magma. This Workshop Volume.

Mitchell RH 1986. Kimberlites. Plenum Press, New York, 441 p.

Mysen, B.O. Structure & Properties of Silicate Melts. Elsevier, Amsterdam (1988).

Plazek DJ & Ngai KL 1991. Correlation of polymer segmental chain dynamics with temperature-dependent time-scale shifts. Macromolecules 24:1222-1224.

Price S Russell JK & Kopylova MK 2000. Primitve magma from the Jericho pipe, N.W.T., Canada: Constraints on primary kimberlite melt chemistry. J Petrol 41: 789-808.

Quane S & Russell JK 2005. Welding: Insights from high-temperature analogue experiments. J Volc Geoth Res 142: 67-87.

Russell JK & Giordano D 2005. A model for silicate melt viscosity in the System $CaMgSi_2O_6$-$CaAl_2Si_2O_8$-$NaAlSi_3O_8$. Geochim Cosmochim Acta 69: 5333-5349.

Russell JK & Quane S 2005. Rheology of welding: Inversion of field constraints. J Volc & Geoth Res 142:173-191.

Sparks RSJ Baker L Brown RJ Field M Schumacher J Stripp G & Walters A 2006 Dynamical constraints on kimberlite volcanism. J Volc & Geoth Res 155:18-48.

Contact: Kelly Russell, Department of Earth and Ocean Sciences, University of British Columbia, 6339 Stores Rd., Vancouver, BC, Canada, V6T 1Z1, E-mail: krussell@eos.ubc.ca

Table 1. Estimates of kimberlite melt compositions from literature and computed transport properties for anhydrous melts. Includes 2 non-kimberlite melts.

	Sparks et al. 2006					*Kopylova et al. (2006, 296-)*				Non-Kimberlite	
Label	*S1*	*S2*	*S3*	*S4*	*S5*	*E-A*	*E-B*	*G-A*	*G-C*	*PD*[1]	*EB*[2]
SiO_2	33.60	35.66	32.73	29.56	34.35	35.79	33.08	32.55	34.73	46.68	48.40
TiO_2	3.76	0.76	1.82	3.82	1.79	1.65	1.72	2.02	1.97	0.18	1.66
Al_2O_3	3.34	1.83	2.67	2.74	2.82	2.22	2.14	2.86	1.95	4.96	16.76
Cr_2O_3	0.27	0.00	0.00	0.26	0.00	0.44	0.35	0.46	0.45	0.37	0.00
FeO(T)	14.05	7.97	10.90	11.24	9.80	8.94	8.45	8.26	8.98	8.78	10.42
MnO	0.31	0.19	0.00	0.22	0.18	0.21	0.21	0.21	0.22	0.00	0.21
MgO	24.80	29.35	32.73	30.80	36.88	34.44	32.41	31.71	34.90	32.22	5.32
CaO	16.14	22.46	14.55	17.73	12.45	13.70	18.72	18.36	14.80	6.49	10.78
Na_2O	0.29	0.37	0.00	0.07	0.35	0.11	0.15	0.13	0.11	0.00	3.86
K_2O	1.96	0.54	2.42	1.35	0.92	1.77	1.77	2.27	1.44	0.33	2.00
P_2O_5	1.48	0.87	2.18	2.21	0.46	0.74	0.99	1.16	0.45	0.00	0.61
NBO/T	3.42	3.97	4.19	4.40	3.94	3.79	4.21	4.08	3.97	2.26	0.71
Tg (°C)[3]	669	742	714	703	719	719	734	735	720	704 (732)	695 (673)
A-VFT[4]	-4.56	-4.56	-4.56	-4.56	-4.56	-4.56	-4.56	-4.56	-4.56	-4.56	-4.56
B-VFT	4708	4787	5125	4932	5214	5156	4968	4908	5150	5104	5557
C-VFT	711	693	712	734	713	700	713	718	708	643	601
Log η (Pas)[5]	1.62	1.58	2.17	2.11	2.30	2.11	1.98	1.94	2.17	1.59	1.81
Tg= 10^{12} Pa s	722	709	748	759	755	738	740	742	746	678	664
M[7]	58.0	56.3	54.6	57.4	54.1	53.8	55.9	56.7	54.2	51.1	46.2

[1]Peridotite (Dingwell et al. 2003); [2]Basalt (Giordano & Dingwell 2003); [3]Tg values predicted by calorimetry (direct measurements in brackets); [4]Calculated VFT parameters: log η= A + B/[T(K)-C] [5]log η @ 1200 °C; [6]Tg computed as the T(°C) where log η =10^{12} Pas; [7]Melt fragility (steepness index)

Table 2. Estimates of volatile-enriched kimberlite melt compositions from literature and transport properties for volatile enriched melts. Includes 2 non-kimberlite melts.

	Sparks et al. 2006					*Kopylova et al. (2006, 296-)*				Non-Kimberlite	
Label	*S1*	*S2*	*S3*	*S4*	*S5*	*E-A*	*E-B*	*G-A*	*G-C*	*PD*[1]	*EB*[2]
SiO_2	28.75	28.63	27.82	28.03	32.13	29.47	26.64	26.45	28.54	46.68	47.29
TiO_2	3.22	0.61	1.55	3.62	1.67	1.35	1.38	1.64	1.62	0.18	1.62
Al_2O_3	2.86	1.47	2.27	2.60	2.64	1.82	1.73	2.33	1.60	4.96	16.37
Cr_2O_3	0.23	0.00	0.00	0.25	0.00	0.36	0.28	0.38	0.37	0.37	0.00
FeO(T)	12.02	6.40	9.27	10.66	9.17	7.36	6.80	6.71	7.38	8.78	10.18
MnO	0.27	0.15	0.00	0.21	0.17	0.17	0.17	0.17	0.18	0.00	0.20
MgO	21.22	23.57	27.82	29.20	34.50	28.35	26.10	25.77	28.68	32.22	5.20
CaO	13.81	18.04	12.37	16.81	11.65	11.28	15.08	14.92	12.16	6.49	10.53
Na_2O	0.25	0.30	0.00	0.07	0.33	0.09	0.12	0.11	0.09	0.00	3.77
K_2O	1.68	0.43	2.06	1.28	0.86	1.46	1.43	1.85	1.19	0.33	1.95
P_2O_5	1.27	0.70	1.85	2.10	0.43	0.61	0.80	0.94	0.37	0.00	0.59
CO_2	7.00	13.02	7.00	0.26	6.45	8.27	11.35	11.16	9.29	0.00	0.00
H_2O	7.44	6.68	8.00	4.92	0.00	9.40	8.14	7.57	8.52	0.00	2.29
NBO/T	4.9	5.3	5.9	5.4	3.9	5.7	6.0	5.7	5.7	2.3	0.95
A-VFT[4]	-4.6	-4.6	-4.6	-4.6	-4.6	-4.56	-4.56	-4.56	-4.56	-4.56	-4.56
B-VFT	5496	5476	5912	5545	5214	6035	5755	5666	5989	5104	5530
C-VFT	633	635	655	657	713	648	666	662	660	643	432
Log η (Pas)[5]	1.98	1.97	2.66	2.24	2.30	2.75	2.57	2.43	2.80	1.59	0.75
Tg= 10^{12} Pa	691	692	739	719	755	739	740	731	748	678	492
M[7]	48.1	48.3	46.9	49.1	54.1	46.0	48.3	48.6	46.8	51.1	38.0

[1]Peridotite (Dingwell et al. 2003); [2]Basalt (Giordano & Dingwell 2003); [3]Tg values predicted by calorimetry (bracketed values are direct measurements); [4]Calculated VFT parameters: log η= A + B/[T(K)-C]; [5]log η @ 1200 °C; [6]Tg is T(°C) where log η =10^{12} Pas; [7]Fragility